

# Numerical Flow Simulation around HSP Propeller in Open Water and behind a Vessel Wake Using RANS CFD Code

Kadda Boumediene, Mohamed Bouzit

**Abstract**—The prediction of the flow around marine propellers and vessel hulls propeller interaction is one of the challenges of Computational fluid dynamics (CFD). The CFD has emerged as a potential tool in recent years and has promising applications. The objective of the current study is to predict the hydrodynamic performances of HSP marine propeller in open water and behind a vessel. The unsteady 3-D flow was modeled numerically along with respectively the  $K-\omega$  standard and  $K-\omega$  SST turbulence models for steady and unsteady cases. The hydrodynamic performances such as a torque and thrust coefficients and efficiency show good agreement with the experiment results.

**Keywords**—Seiun Maru propeller, steady, unsteady, CFD, HSP.

## NOMENCLATURE

$J$ [-]	Advance coefficient
$KT$ [-]	Thrust coefficient
$KQ$ [-]	Torque coefficient
$V_a$ [m/s]	Propeller advance velocity
$Re$ [-]	Reynolds number
$C_p$ [-]	Propeller pressure coefficient
$n$ [rps]	Propeller revolution
$D$ [m]	Propeller diameter
$V_0$ [Knots]	Vessel speed
$P$ [m]	Propeller Pitch
$\eta_0$ [-]	Propeller efficiency in open water

## I. INTRODUCTION

PROPELLER generally runs in the stern of the vessel. This area is in the hull where a periodic and fluctuating pressure is generated by the inflow [11]. Vibratory forces occur as a result of said fluctuating pressure. The vibrations are transferred to the hull of the vessel directly through the shaft-line. Both crew and passengers are disturbed and feel uncomfortable while the vibrations are occurring. Therefore, it is extremely difficult for hydro-dynamists and naval architects to foretell the vessel's propeller performance operating in the vessel's hull stern. A large number of studies based on experiments and numerical researches have been carried out to predict propeller hydrodynamic performances in open water and behind a vessel stern [5], [8], [9]. In the recent years, many numerical methods based on solving Reynolds-Averaged Navier-Stokes equations

have made remarkable progress and widely applied to address problem in vessel hydrodynamic [1].

The article provides a numerical simulation of steady and unsteady turbulent flow in non-cavitating case around the Seiun Maru HSP propeller [13]. This work attempts to reproduce the hydrodynamic characteristics such as thrust, torque and pressure coefficients in open water and behind a ship hull. The commercial code Ansys Fluent 6.3.26 was used based on the finite volume method by means of the RANS approach. The turbulence models  $K-\omega$  standard and  $K-\omega$  SST [2] were chosen for the simulation of both steady and unsteady flow. The results obtained are in a good agreement with the experiment results.

## II. PROPELLERS CHARACTERISTICS

The Seiun Maru HSP propeller is chosen as a reference case for experiment benchmark and CFD analysis [4]. HSP [13] is a variable pitch propeller with 5 blades, designed in Japan and has taken the name of Seiun Maru vessel. The geometry and the characteristics of the propeller are shown in Table I and Fig. 1.

TABLE I  
 MAIN CHARACTERISTICS OF THE SEIUN MARU HSP PROPELLER

Propeller Full scale	HSP
Number of Blades [-]	5
Diameter [m]	3.6
Boss Ratio [-]	0.1972
Pitch [-]	Variable
Expanded Area Ratio [-]	0.7
Rake [Deg]	-3.03
Skew at R [m]	1.3367
Material [-]	Ni-Al-Bz



Fig. 1 Geometry of the Seiun Maru HSP propeller

Kadda Boumediene and Mohamed Bouzit are with the Mechanical Engineering Department University of Science and Technology of Oran-USTO-MB, Oran, Algeria (e-mail: kadda.boumediene@univ-usto.dz, mohamed.bouzit@univ-usto.dz).

### III. PROPELLER DRAWING PROCEDURES

To generate the geometry of the propeller, a FORTRAN program was used based on the geometric characteristics of Seium Maru HSP propeller such as rake, skew, chord of the cross-sections [3]. The program transforms input data to points with coordinates in space and these points are exported to preprocessor Gambit to describe the shape of the propeller blade and then can be connected into curves using spline lines. The shaft was connected to the propeller root blades using T junction on Gambit. Fig. 2 shows the propeller drawing steps.

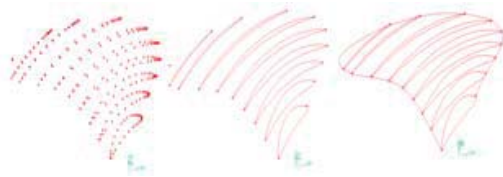


Fig. 2 The propeller drawing steps

### IV. MESH GENERATION AND BOUNDARY CONDITIONS

For both steady and unsteady case, an unstructured mesh was generated using GAMBIT. First, the blade surface was meshed with constant triangles cells in all the blade faces approximately  $0.0055D$ . The shaft surface was meshed with triangles cells of  $0.0198D$  as it is shown in Fig. 3.

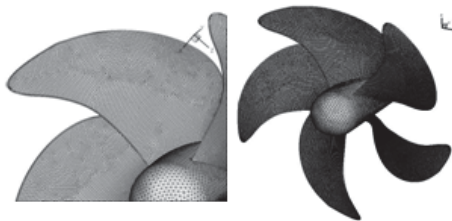


Fig. 3 Propeller surface mesh

The computational domain covers all the 5 blades with 6 rotational blocs, these blocs are connected with interfaces [12].

For the steady case, the inlet boundary is at  $1.5D$  with a uniform inflow of the velocity components, which depends of the advance coefficient  $J$  [7], outlet at  $3.5D$  with a static pressure, and the outer boundary at  $1.4D$  from the shaft axis which represent a slip condition.

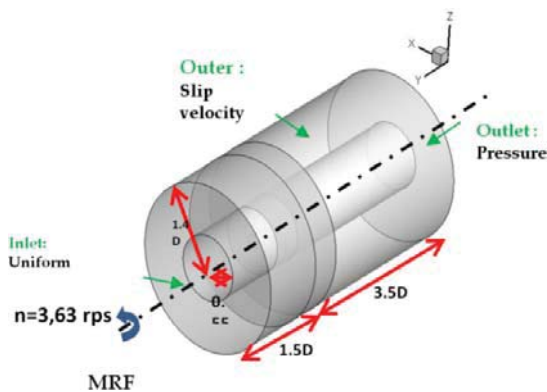


Fig. 4 Computational domain for steady simulation

The non-slip condition was imposed for the blade and hub surfaces. The fluid is considered rotational around the y-axis (shaft axis) using the Moving Reference Frame (MRF) for the steady case.

Figs. 4 and 5 show respectively the computational domain and the mesh generated for the steady case.



Fig. 5 The grid of the domain for steady simulation

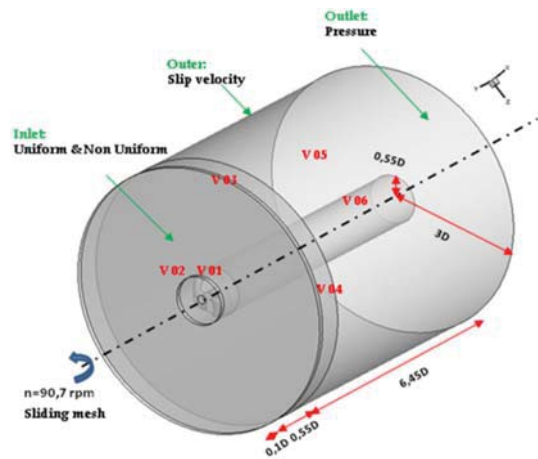


Fig. 6 Computational domain for unsteady simulation, for HSP Seium Maru propeller

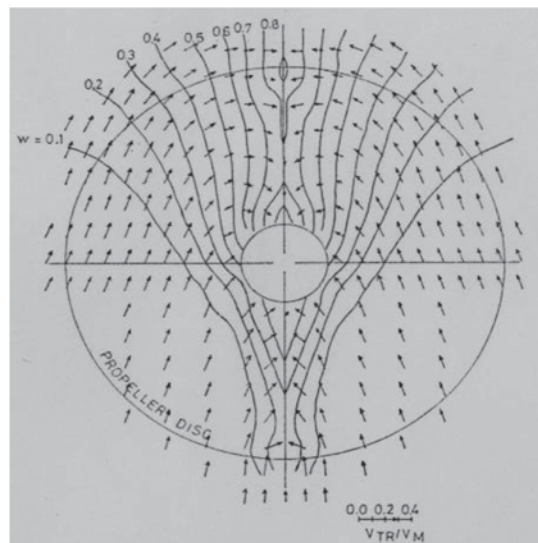


Fig. 7 Nominal wake measured

For the unsteady case, the same computation domain was used, stationary blocs and 2 rotational blocs rotate with the propeller using the sliding mesh technique. The inlet, outlet and radial boundaries were located at  $0.35D$ ,  $6.7D$ ,  $3D$  from the center of the propeller as it is shown in Fig. 6.

The same boundary conditions were used as the steady case, only the exception is at the inlet of the small stationary cylinder where the axial components of the velocity calculated from the measured nominal wake were imposed. Tetra cells were used with the same mesh method as the steady domain with a local nodes distribution on the edges to control the mesh. The number of cells is estimated at 2 000 000.

### V. MATHEMATICAL FORMULATION

The turbulent viscous flow around the propeller is described by the Navier-Stokes and turbulent equations as follows:

$$\frac{\partial u_i}{\partial x_i} = 0 \quad (1)$$

$$\frac{\partial(\rho u_i)}{\partial t} + \frac{\partial(\rho u_i u_j)}{\partial x_j} = -\frac{\partial P}{\partial x} + \frac{\partial}{\partial x_j} \left( \mu \frac{\partial u_i}{\partial x_j} - \overline{\rho u_i' u_j'} \right) \quad (2)$$

#### A. The Standard $k - \omega$ Turbulence Model

The Wilcox [2]  $k-\omega$  two-equation model is given by the following turbulent kinetic energy and dissipation equations:

$$\frac{\partial(\rho k)}{\partial t} + \frac{\partial(\rho u_j k)}{\partial x_j} = P - \beta^* \rho \omega k + \frac{\partial}{\partial x_j} \left[ \left( \mu + \sigma_k \frac{\rho k}{\omega} \right) \frac{\partial k}{\partial x_j} \right] \quad (3)$$

$$\frac{\partial(\rho \omega)}{\partial t} + \frac{\partial(\rho u_j \omega)}{\partial x_j} = \frac{\gamma \omega}{k} P - \beta \rho \omega^2 + \frac{\partial}{\partial x_j} \left[ \left( \mu + \sigma_\omega \frac{\rho k}{\omega} \right) \frac{\partial \omega}{\partial x_j} \right] + \frac{\rho \sigma_d}{\omega} \frac{\partial k}{\partial x_j} \frac{\partial \omega}{\partial x_j} \quad (4)$$

Explicit details for the model can be found in [9] and [10].

### VI. NUMERICAL PROCEDURES

The commercial code Ansys Fluent 6.3.26 based on the finite volume method was used. The Reynolds Navier Stokes Equation for incompressible flow was applied for both steady and unsteady flow simulation. The turbulence models  $k-\omega$  and  $K-\omega$  SST [2] were used respectively for steady and unsteady flow. Segregated solvers SIMPLE and PISO as the velocity-coupling algorithm were chosen respectively for both steady and unsteady simulation. QUICK scheme was adopted for the discretization of diffusion and convection terms of the momentum equation and STANDARD scheme was chosen to discretization the continuity equation. UPWIND first order scheme was selected for the discretization of the equations of turbulent energy and dissipation. Relaxation factors were adjusted during the simulation and the condition of non-uniform inflow characterized by the wake field calculated by Sasajima and Tanaka method in towing tank was implemented in Fluent.

### VII. TEST CONDITIONS

The simulation for the steady case was carried out for a Seiun Maru model with a scale of 1/9 to match the conditions of the experiment done by Ukon [6] in the open water tests, with a

rotation  $n=3.63$  rps ( $Re=5.8 \cdot 10^5$ ) and a diameter of propeller  $D=0.4$  m. However, for the unsteady case, the simulation is achieved for a full-scale propeller with a diameter  $D=3.6$  m, rotation of HSP propeller was set  $n=90.7$  rpm and a vessel speed  $V_0=9.0$  knots.

### VIII. RESULTS IN OPEN WATER CHARACTERISTICS

The results are compared with the experiments. The simulation was achieved for a computer i7 2.4 GHZ 4GO RAM, using the parallel method for each advance coefficient case J.

Fig. 8 shows the curves of  $K_T$  and  $K_Q$  of HSP propeller compared with the experiments results. The red lines show the numerical results obtained from the simulation, the green lines are the experiments results find by Ukon in the open water tests. The results obtained are in a good agreement compared with the experiment for a wide range of advance coefficient.

### IX. RESULTS SIMULATION BEHIND A VESSEL HULL

The simulation of unsteady flow in non-uniform vessel wake was carried out for HSP [13] using the sliding mesh technique. The time step was set to 0.00183756 for HSP [13] which correspond to the rotation angle of 1 degree.

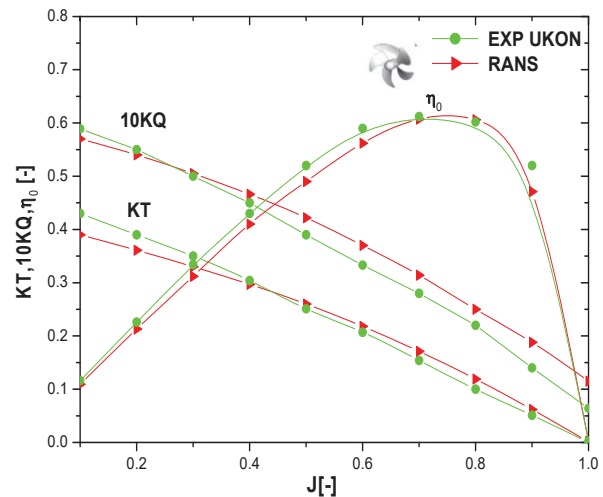


Fig. 8 Open water characteristics of Sein Maru HSP propeller

Fig. 9 shows the pressure distribution on the blade suction and pressure sides at 180 degrees, it is clear that pressure changes on depending on the blade position due to the non-uniform inflow.

Fig. 10 shows chord wise distribution of the pressure coefficient at 0.7R and 0 degree. Fig. 10 shows the variation of the pressure coefficient of HSP Seiun Maru Propeller at 0.7R and  $x/c=10\%$  during a rotation of the propeller. The results obtained are in a good agreement with the experiment carried out by Ukon.



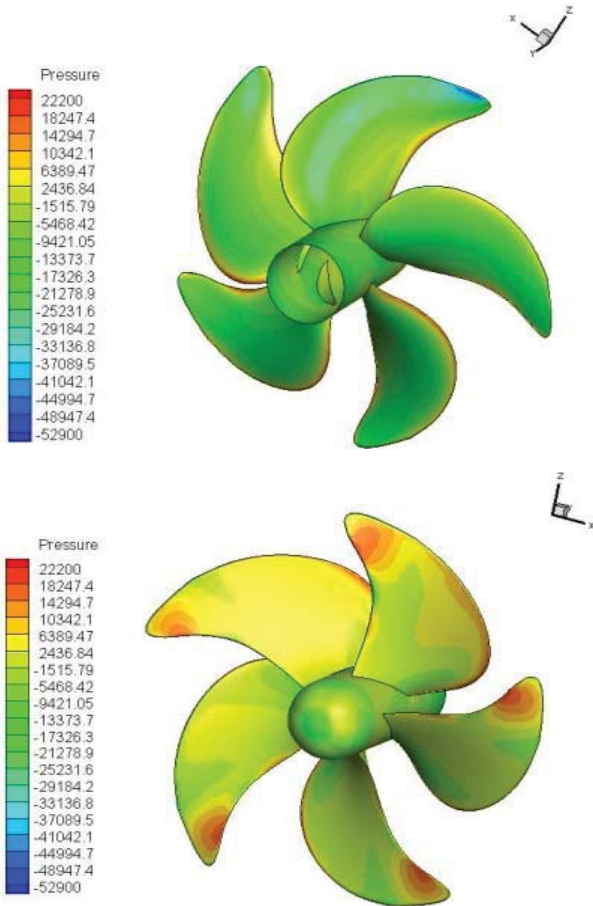


Fig. 9 Pressure contours for Seiu Maru HSP

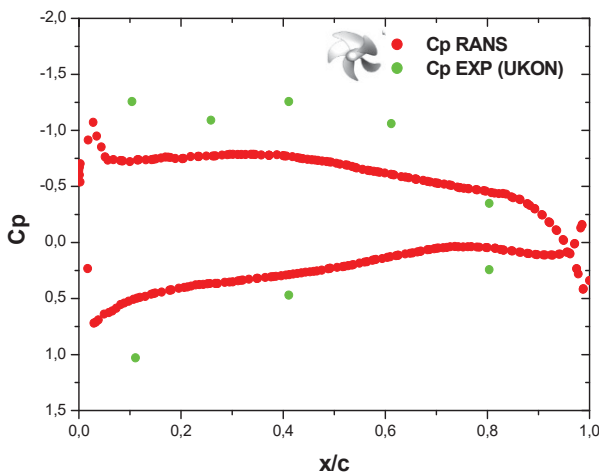


Fig. 10 Chordwise distribution of the pressure

Fig. 11 shows the thrust coefficient  $K_T$  for one and five blades of the Seiu Maru HSP [13] during on revolution. The Green triangles are the experiment results and the red are the numerical results. It is a clear that the fluctuation of  $K_T$  is important for CP however, it is smaller for HSP [13]. The Seiu Maru CP has a bigger thrust coefficient  $K_T$  than HSP and it is estimated respectively by 0.211 and 0.197. The error of  $K_T$  was estimated by 3.9% for HSP [13].

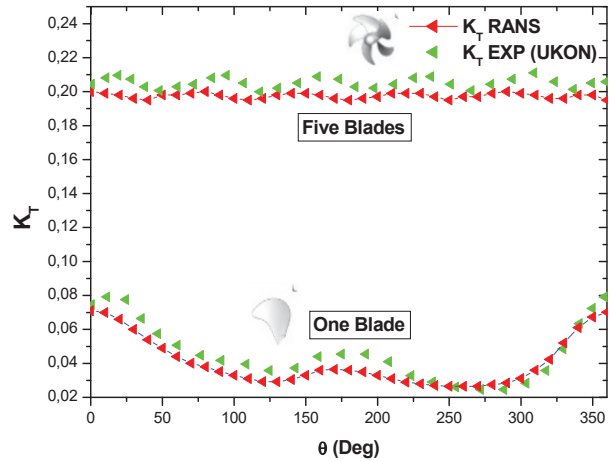


Fig. 11 Thrust coefficient for Seiu Maru HSP during one revolution

## X. CONCLUSION

This work is a contribution to the numerical study of turbulent flow around Seiu Maru marine propeller in steady and unsteady case. The aim of this work is to propose a method for best efficiency prediction. First, a steady simulation conducted for a wide range of advance coefficient of  $J$  between 0.1 and 1 was carried out for HSP propeller [13] to predict the open water characteristics such as thrust torque coefficients and the efficiency of the propeller. The standard  $K-\omega$  model was selected for the steady case with the moving reference frame option (MRF). The results obtained agree well with the experiment and the error of  $K_T$  was estimated respectively for HSP propeller [13] by 2% and 6% while the error of  $K_Q$  was 6.5% and 6%.

The second part is an unsteady simulation in a non-uniform vessel wake to calculate the thrust during propeller revolution.  $K-\omega$  SST [2] model was selected and the sliding mesh technique was used. It was clear that the pressure distribution change depends on the blade position. The thrust coefficient calculated during propeller revolution agrees well with the experiment. The time step corresponds to a rotation angle of 1 degree.

## REFERENCES

- [1] Vessel resistance and propulsion practical estimation of vessel propulsive power de Anthony F. Molland, Professor Stephen R. Turnock, Dominic A. Hudson, 1<sup>st</sup> Edition, ISBN 978-0-521-76052-2 (hardback) 2011.
- [2] Wilcox, D. C., Turbulence Modeling for CFD, 2nd Ed., DCW Industries, Inc., La Canada, CA, 1998.
- [3] Marine propeller and propulsion John Carlton, 2<sup>nd</sup> Edition Great Britain, MPG Books Ltd, Bodmin Cornwall, 2007.
- [4] Funeno, I., "On Viscous flow around Marine Propellers- Hub Vortex and Scale Effect", *Proceedings of New-S-Tech 2002 (Third Conference for New Vessel and Marine Technology) 2002*, pp.17-26.
- [5] Krasilnikov "Analysis of Unsteady Propeller Blade Forces by RANS" Norwegian Marine Technology Research Institute (MARINTEK), Trondheim Norway June 2009.
- [6] Ukon, Y., Kurobe, Y. and Kudo, T., "Measurement of pressure distribution on a conventional and highly skewed propeller model – under non cavitating condition- (in Japanese)", *Journal of the society of naval architects of Japan*, Vol.165, 1989, pp.83-94.
- [7] L.d. Qing "Validation of RANS Predictions of Open Water Performance of a Highly Skewed Propeller with Experiments" *Conference of Global Chinese Scholars on Hydrodynamics*.

- [8] Martin Visohlyd, Krishnan Mahesh "Large Eddy Simulation of Crashback in Marine Propellers" *University of Minnesota, Minneapolis, MN 55455 American institut of Aeronotics and Astronautics 2006-1414.*
- [9] Wilcox, D. C., 2006, *Turbulence Modeling for CFD*, 3rd Ed., DCW, Industries, Inc., La Canada, CA.
- [10] Menter, F., 1994. Two-equation eddy- viscosity turbulence model for engineering applications, *AIAAJ.*, 32(8):1598-1605.
- [11] *Architecture Navale connaissance et pratique Dominique Presles édition de la villette, ISBN 2-915456-14-3.*
- [12] A. Califano, S. Steen "Analysis of different Propeller ventilation mechanisms by means of RANS" *First international symposium on marine Propulsors smp'09, Trondheim, Norway, June 2009.*
- [13] Bureau Veritas, "Rules for the Classification of Steel Vessels - Part C Machinery, Electricity, Automation and Fire Protection" *Part C, Chap1, Section 8 Propellers pp148-155. BV July 2014.*